

# Chapter 11

## Radioimmuno-detection of Atherosclerotic Lesions Focusing on the Accumulation Mechanism of Immunoglobulin G

Yoichi Shimizu, Hiroko Hanzawa, Yan Zhao, Ken-ichi Nishijima, Sagiri Fukura, Takeshi Sakamoto, Songji Zhao, Nagara Tamaki, and Yuji Kuge

**Abstract** In the diagnosis of atherosclerosis, detailed evaluation of biomarkers related to its lesion formation is desired for estimation of its progression rate. In our previous proteomic studies of atherosclerosis mice, the protein level of thrombospondin-4 (TSP4) in the aorta, but not in plasma, elevated relatively with atherosclerotic plaque formation. Therefore, we supposed that TSP4 would be a potential biomarker for diagnostic imaging of atherosclerotic progression. Immunoglobulin G (IgG) has been widely used as a basic molecule of imaging probes providing images specific to their target biomolecules, owing to the antigen-antibody reaction. Therefore, we first developed anti-TSP4 monoclonal IgG radiolabeled with  $^{99m}\text{Tc}$  ( $^{99m}\text{Tc}$ -TSP4-mAb).  $^{99m}\text{Tc}$ -TSP4-mAb showed higher accumulation in atherosclerotic aortas of apoE<sup>-/-</sup> mice (atherosclerotic model

---

Y. Shimizu (✉)

Faculty of Pharmaceutical Sciences, Hokkaido University, Sapporo, Japan

Central Institute of Isotope Science, Hokkaido University, Sapporo, Japan

Graduate School of Medicine, Hokkaido University, Sapporo, Japan

e-mail: [yshimizu@pharm.hokudai.ac.jp](mailto:yshimizu@pharm.hokudai.ac.jp)

H. Hanzawa • T. Sakamoto

Research & Development Group, Hitachi, Ltd., Kokubunji, Tokyo, Japan

Y. Zhao • S. Fukura • S. Zhao

Graduate School of Medicine, Hokkaido University, Sapporo, Japan

K. Nishijima

Central Institute of Isotope Science, Hokkaido University, Sapporo, Japan

Graduate School of Medicine, Hokkaido University, Sapporo, Japan

N. Tamaki

Department of Nuclear Medicine, Graduate School of Medicine, Hokkaido University, Sapporo, Japan

Y. Kuge

Central Institute of Isotope Science, Hokkaido University Department of Integrated Molecular Imaging, Graduate School of Medicine, Hokkaido University, Sapporo, Japan

mice); however, we found that the non-targeted monoclonal IgG radiolabeled with  $^{99m}\text{Tc}$  also showed similar distribution in atherosclerotic aortas of apoE $^{-/-}$  mice. IgG has also known to accumulate nonspecifically in the immunological disease such as inflammatory arthritis. However, the accumulation mechanism of IgG has still been unclear in detail. In this chapter, we would like to introduce recent topics on atherosclerotic imaging, focused on our work exploring the accumulation mechanisms of IgG in atherosclerotic lesions, and elucidating the usefulness of radiolabeled IgG images in the diagnosis of atherosclerosis.

**Keywords** Atherosclerosis • Immunoglobulin G • Polarized macrophage

## 11.1 Introduction

Rupture of vulnerable plaques and the subsequent thrombogenesis induce ischemic diseases such as cerebral and myocardial infarction [1]. Therefore, it is necessary to detect vulnerable lesions precisely for the diagnosis of such diseases. Various biomolecules are expressed or activated as atherosclerosis progresses. Thus, the detection and imaging of such biomolecules would make possible the determination of the progression of atherosclerosis in detail. In our previous proteomic studies of atherosclerotic model mice [2], the relative thrombospondin-4 (TSP4) levels of atherosclerotic model mice/normal mice in the aorta, but not in plasma, increased with the atherosclerotic plaque formation. TSP4 belongs to the thrombospondin families and has been reported to play some roles such as promotion of proliferation of smooth muscle cells and adhesion and migration of neutrophils [3]. It has also been reported that apoE and TSP4 double knockout mice showed fewer atherosclerotic lesions than the atherosclerosis apoE knockout mice, which suggests that TSP4 has a crucial role in the progression of atherosclerotic lesions [4]. Therefore, we supposed that TSP4 would be a potential biomarker for diagnostic imaging of atherosclerotic progression. Immunoglobulin G (IgG) is widely used particularly for the target-specific imaging of cancer, because it provides images specific to their target biomolecules owing to the antigen-antibody reaction [5]. Thus, we first developed an IgG-based TSP4 targeting SPECT imaging probe ( $^{99m}\text{Tc}$ -TSP4-mAb).  $^{99m}\text{Tc}$ -TSP4-mAb accumulated in the atherosclerotic lesions of apoE $^{-/-}$  mouse aortas. However,  $^{99m}\text{Tc}$ -NC-mAb, which was composed of non-targeting IgG, also accumulated highly in the atherosclerotic lesions similar to  $^{99m}\text{Tc}$ -TSP4-mAb. IgG itself is known to be delivered to atherosclerotic lesions nonspecifically, but the detailed mechanism of the accumulation is still unknown [6].

In this report, we would like to introduce our above-mentioned work in which we explored the accumulation mechanisms of IgG in atherosclerotic lesions and elucidated the usefulness of radiolabeled IgG imaging in the diagnosis of atherosclerosis.

## 11.2 Materials and Methods

### 11.2.1 Materials

All chemicals used in this study were commercially available and of the highest purity. HYNIC-N-hydroxysuccinimide was prepared as previously reported [7].  $^{99m}\text{Tc}$ -pertechnetate was purchased from Nihon Medi-Physics Co., Ltd. (Tokyo, Japan). As a TSP4-targeting monoclonal antibody, we used anti-thrombospondin-4 mouse IgG<sub>2b</sub> (Clone #276523, R&D Systems, Abingdon, UK). As for the negative control non-targeted mouse IgG, we chose mouse IgG<sub>2b</sub>, a kappa monoclonal [MG2b-57] isotype control (Abcam, Cambridge, UK) whose immunogen is trinitrophenol + keyhole-limpet hemocyanin (KLH).

### 11.2.2 Preparation of Radiolabeled IgG

Anti-TSP4 monoclonal IgG (TSP4-mAb) or non-targeting IgG (NC-mAb) was radiolabeled with  $^{99m}\text{Tc}$  after derivatization with 6-hydrazinonicotinic acid (HYNIC), as previously reported (Fig. 11.1) [8]. In brief, to HYNIC-N-hydroxysuccinimide (8.25  $\mu\text{g}$ ) in *N,N*-dimethylformamide (8.25  $\mu\text{l}$ ), TSP4-mAb or NC-mAb solution in 0.16 M borate buffer (pH 8.0) (250  $\mu\text{l}$ , 2 mg/ml) was added, and the

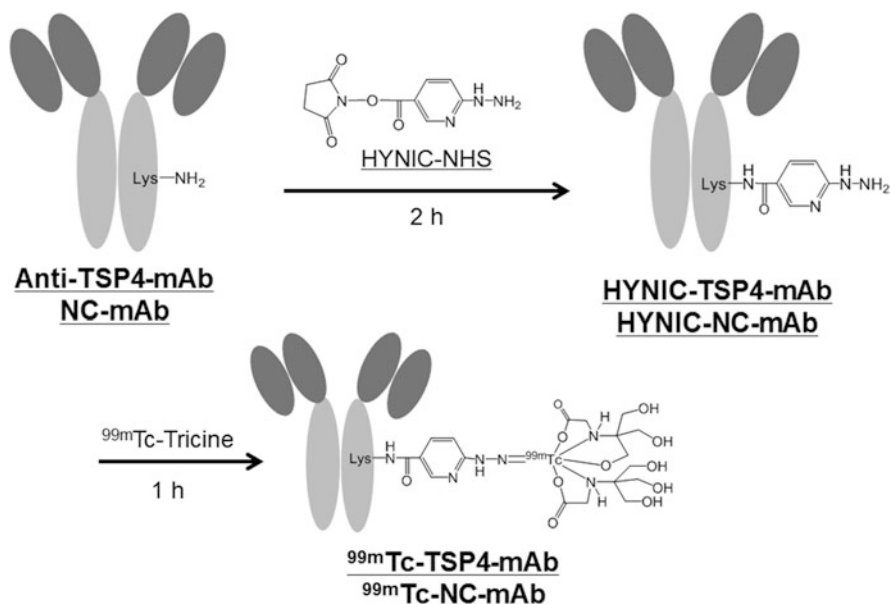


**Fig. 11.1** Scheme of  $^{99m}\text{Tc}$ -TSP4-mAb or  $^{99m}\text{Tc}$ -NC-mAb preparation

mixture was incubated at room temperature for 2 h. The mixture was purified by size-exclusion filtration using a diafiltration membrane (Amicon Ultra 4 [cutoff molecular weight, 30,000]; Millipore Co., Billerica, MA).  $^{99m}\text{Tc}$ - $(\text{tricine})_2$  (740 MBq/ml, 300  $\mu\text{l}$ ) was prepared by the method of Larsen et al. [9]. It was added to the purified solution of HYNIC-TSP4-mAb or NC-mAb solution in 10 mM citrate buffer (pH 5.2) (30  $\mu\text{l}$ , 1 mg/ml), and the mixture was incubated at room temperature for 1 h. The mixture was then purified on a Sephadex G-25 column (PD-10, GE Healthcare, Buckinghamshire, UK) equilibrated with 0.1 M PBS (pH 7.4) to obtain  $^{99m}\text{Tc}$ -TSP4-mAb or  $^{99m}\text{Tc}$ -NC-mAb. The radiochemical purity of  $^{99m}\text{Tc}$ -TSP4-mAb or  $^{99m}\text{Tc}$ -NC-mAb was measured by size-exclusion filtration of the PD-10 column and size-exclusion high-performance liquid chromatography (HPLC). The stability of  $^{99m}\text{Tc}$ -TSP4-mAb or  $^{99m}\text{Tc}$ -NC-mAb in plasma was evaluated by the method described below. First, the probes ( $^{99m}\text{Tc}$ -TSP4-mAb, 27.7 MBq/ml;  $^{99m}\text{Tc}$ -NC-mAb, 34.9 MBq/ml; 50  $\mu\text{l}$ ) were incubated with the plasma derived from C57BL/6 (male, 30 weeks) for 24 h, and then the mixture was analyzed by size-exclusion filtration of the PD-10 column.

### 11.2.3 Animal Study

Animal care and all experimental procedures were performed with the approval of the animal care committee of Hokkaido University. Studies were performed using male C57BL/6J apoE<sup>-/-</sup> mice obtained from the Taconic Gnotobiotic Center (Germantown, NY, USA) and C57BL/6J mice as the wild-type (WT) mice obtained from Charles River Laboratories Japan, Inc. (Yokohama, Japan). The animals were kept in a temperature-controlled facility of the laboratory of animal experiments of Hokkaido University on a 12-h light cycle with free access to food and water. After 5 weeks of age, the apoE<sup>-/-</sup> mice were maintained on a high-fat diet (21 % fat, 0.15 % cholesterol, without cholate; purchased from Oriental Yeast Ltd., Tokyo, Japan). At 35 weeks of age, the animals ( $n = 4/\text{group}$ ) were anesthetized with pentobarbital (0.025 mg/kg body weight, intraperitoneally).  $^{99m}\text{Tc}$ -TSP4-mAb (200–592 kBq/mouse) or  $^{99m}\text{Tc}$ -NC-mAb (481–962 kBq/mouse) was intravenously injected to each animal. Twenty-four hours after the injection, the animals were euthanized under deep pentobarbital anesthesia, and aortas were fixed by cardiac perfusion with cold 0.1 M phosphate-buffered saline (pH 7.4) followed by a cold fixative [4 % paraformaldehyde, 0.1 M phosphate-buffered solution (pH 7.4)]. Each excised aorta was cut and placed onto glass slides. The dissected aortic root of each mouse was embedded in Tissue-Tek medium (Sakura Finetechnical Co., Ltd., Tokyo, Japan) and frozen in isopentane/dry ice. Serial cross sections of 10- $\mu\text{m}$  (for autoradiographic study) and 5- $\mu\text{m}$  (for immunohistochemical analysis) thickness were immediately cut and thaw-mounted on glass slides.

### 11.2.3.1 Autoradiography (ARG) Study

The excised and cut aortas on glass slides were exposed to phosphor imaging plates (Fuji Imaging Plate BAS-UR, Fujifilm, Tokyo, Japan) for 12 h, together with a set of calibrated standards. The autoradiographic images were acquired using a computerized imaging analysis system (Fuji bio-imaging analyzer FLA7000). The acquired data was analyzed using MultiGauge version 3.2 (Fujifilm).

### 11.2.4 Histochemical Study

Movat's pentachrome staining of serial aortic root sections was performed [10]. Immunohistochemical staining of the serial sections with a mouse macrophage-specific antibody (Mac-2, clone m3/38, Cedarlane, Ontario, Canada) was performed in accordance with a previously reported immunohistochemical procedure [11]. The TSP4 immunohistochemical staining of the serial sections was performed as shown below. At first, endogenous peroxidase activity was blocked for 10 min with 3 % hydrogen peroxide after rehydration. Slides were then incubated with anti-thrombospondin-4 mouse IgG<sub>2b</sub> (Clone #276523, R&D Systems) overnight at 4 °C, followed by incubation with a peroxidase-labeled amino acid polymer-conjugated goat anti-mouse F(ab')<sub>2</sub> fragment of IgG (Histofine Mouse Stain kit, Nichirei, Tokyo, Japan) for 30 min at room temperature. The bound antibody complex was then visualized by incubation with 3,3'-diaminobenzidine tetrahydrochloride. The images of the staining shown above were captured under a microscope (Biozero BZ-8000; Keyence Co., Osaka, Japan).

## 11.3 Results

### 11.3.1 Probe Preparation

<sup>99m</sup>Tc-TSP4-mAb or <sup>99m</sup>Tc-NC-mAb was obtained with a radiochemical yield of 17.6 ± 3.8 % or 31.8 ± 6.8 % (n = 3) and with the radiochemical purity of 99.5 ± 0.1 % or 99.2 ± 0.5 % (n = 3). The stability of <sup>99m</sup>Tc-TSP4-mAb or <sup>99m</sup>Tc-NC-mAb in the mouse plasma was over 90 % for 24-hour incubation.

### 11.3.2 In Vivo Study

The distributions of <sup>99m</sup>Tc-TSP4-mAb in apoE<sup>-/-</sup> mice and wild-type (WT) mice at 24 h after administration are shown in Table 11.1. The <sup>99m</sup>Tc-TSP4-mAb

**Table 11.1** Biodistribution of  $^{99m}\text{Tc}$ -TSP4-mAb in apoE $^{-/-}$  or wild-type (WT) mice 24 h after administration

	apoE $^{-/-}$	WT
Aorta	5.3 ± 1.1	2.4 ± 0.3
Heart	1.8 ± 0.3	1.5 ± 0.2
Lung	1.7 ± 1.4	1.9 ± 1.6
Liver	5.5 ± 1.8	5.9 ± 1.3
Kidney	2.5 ± 0.2	2.3 ± 0.3
Stomach	1.8 ± 0.5	1.1 ± 0.2
Small intestine	1.3 ± 0.2	1.5 ± 0.2
Large intestine	3.8 ± 1.9	2.5 ± 0.3
Pancreas	0.8 ± 0.2	0.7 ± 0.1
Spleen	7.5 ± 1.2	6.7 ± 0.8
Brain	0.1 ± 0.1	0.1 ± 0.0
Muscle	0.5 ± 0.2	0.6 ± 0.1
Blood	17.2 ± 2.1	17.2 ± 1.5

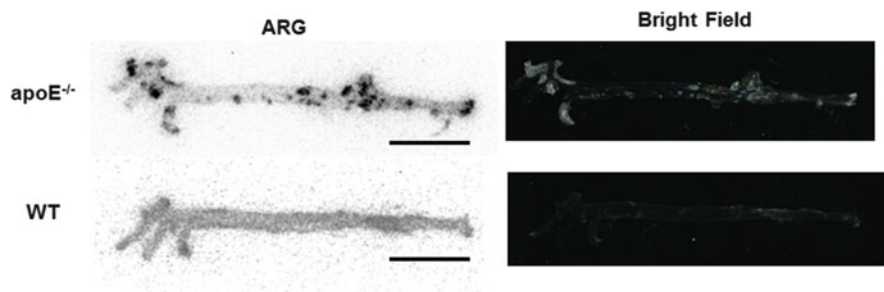


**Fig. 11.2** ARG images (left) and bright field images (right) of the excised aortas of apoE $^{-/-}$  mouse (upper) and of wild-type (WT) mouse (lower) 24 h after administration of  $^{99m}\text{Tc}$ -TSP-mAb

accumulation levels in the aortas of apoE $^{-/-}$  mice were significantly higher than those in WT mice ( $5.3 \pm 1.1$  vs.  $2.4 \pm 0.3$  %ID/g,  $p < 0.05$ ), whereas the radioactivities in other organs were not significantly different between apoE $^{-/-}$  mice and wild mice. On the other hand, the  $^{99m}\text{Tc}$ -NC-mAb accumulation levels in the aortas of apoE $^{-/-}$  mice were also significantly higher than those of WT mice ( $5.1 \pm 1.4$  vs.  $2.8 \pm 0.5$  %ID/g,  $p < 0.05$ ), whereas the radioactivities in other organs were not different between apoE $^{-/-}$  mice and wild-type mice.

The ARG images of the apoE $^{-/-}$  aortas injected with  $^{99m}\text{Tc}$ -TSP4-mAb showed heterogeneous distribution of the radioactivity where the plaque formation was observed in the bright field (Fig. 11.2). The radioactive distribution in the aortic roots of apoE $^{-/-}$  mice injected with  $^{99m}\text{Tc}$ -TSP4-mAb measured by ARG was inside of the atherosclerotic plaque lesions and coincided with the Mac-2-positive areas (Fig. 11.3). These results suggest that  $^{99m}\text{Tc}$ -TSP4-mAb accumulated in the macrophage-infiltrated area of the plaque lesions.

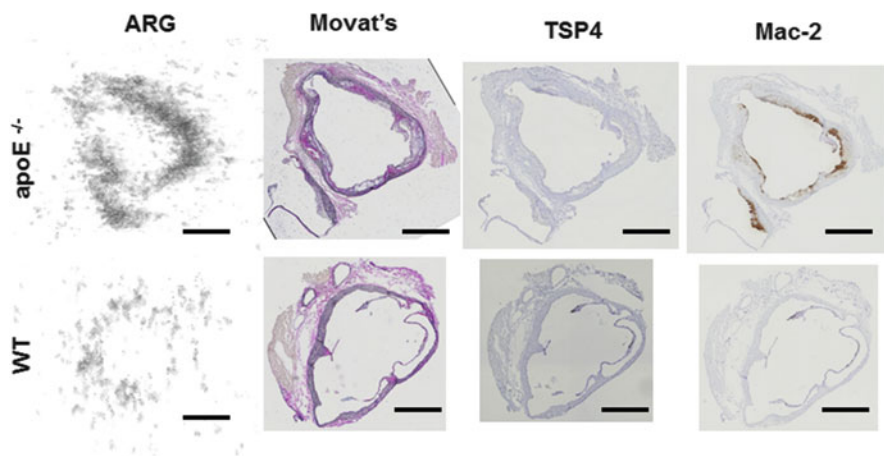


**Fig. 11.3** ARG images, Movat's pentachrome staining, TSP4 immunohistochemical staining, and Mac-2 immunohistochemical staining of the aortic roots of apoE<sup>-/-</sup> mouse (*upper*) and wild-type (WT) (*lower*) mouse 24 h after administration of <sup>99m</sup>Tc-TSP4-mAb

### 11.3.3 Discussion

In this study, we observed that <sup>99m</sup>Tc-TSP4-mAb accumulated in the atherosclerotic lesions of apoE<sup>-/-</sup> mouse aortas. However, <sup>99m</sup>Tc-NC-mAb, which was composed of non-targeting IgG, also accumulated highly in the atherosclerotic lesions similar to <sup>99m</sup>Tc-TSP4-mAb (Fig. 11.2). Moreover, the <sup>99m</sup>Tc-TSP4-mAb accumulation area coincided with the Mac-2-positive areas in the plaques in aortic root (Fig. 11.3), which suggests that IgG itself was delivered and accumulated in atherosclerotic lesions, especially macrophage infiltration areas.

Previously, various types of polarized macrophage were identified and reported [12]. Among the polarized macrophages, pro-inflammatory M1-polarized macrophages were reported to be abundant in lipids and to localize in areas that are distinct from those in which anti-inflammatory M2-polarized macrophages (which are also called alternatively activated macrophages) localize in human plaques [13]. Although the origin of M1 and polarized macrophages and how polarized macrophages are involved in the progression of atherosclerotic plaques are still being unclarified, polarized macrophages would have a critical role in the development of atherosclerotic plaques [14]. Therefore, we examined the correlation of the macrophages, especially polarized macrophages, with IgG accumulation. In our preliminary in vitro study, M1-polarized macrophages showed a higher uptake of <sup>99m</sup>Tc-NC-mAb than M2-polarized and non-polarized M0 macrophages [15]. To clarify the mechanism of <sup>99m</sup>Tc-NC-mAb accumulation in M1-polarized macrophages, we next focus on the expression levels of Fcγ receptors. Fcγ receptors recognize the Fc region of IgG and play a role in the activation of immune systems [16]. Furthermore, it has been reported that deficiency of Fcγ receptors induces

protection against atherosclerosis in apoE<sup>-/-</sup> mice [17]. Indeed, the expression level of some subtypes of Fcγ receptors was higher in M1-polarized macrophages than those in M2-polarized or non-polarized M0 macrophages in our unreported *in vitro* study. We also performed a cellular uptake study under the Fcγ receptor's inhibition and found that the accumulation of <sup>99m</sup>Tc-NC-mAb in M1-polarized macrophages was significantly suppressed by the pretreatment with an anti-Fcγ receptor antibody. These findings suggest that IgG itself is accumulated in M1-polarized macrophages via Fcγ receptors in the atherosclerotic plaques.

During the course of atherosclerotic progression, various biomolecules are expressed or activated. Thus, various PET/SPECT imaging probes targeting biomolecules related to the progression of atherosclerosis have been developed [18]. Among them, some probes are developed with based on monoclonal IgG and have been evaluated in animal models such as mouse and rabbit [19, 20]. In those studies, xenogeneic antibodies were used, whose nonspecific accumulation in atherosclerotic lesions was not taken into consideration. However, considering that the probes will be used clinically, the IgG used as a basic component of probes should be humanized, and it would be necessary to note its nonspecific accumulation as we have seen in this study.

Radiolabeled IgG has been widely applied to the diagnosis of inflammatory diseases such as rheumatoid arthritis and infections, although the mechanism of its accumulation is still unclarified [21]. Our preliminary study is the first to show that pro-inflammatory M1-polarized macrophages contribute to the accumulation of radiolabeled IgG, which is in agreement with the conventional use of such IgG as mentioned above.

In the nuclear imaging for diagnosis of atherosclerosis, 18-fluoro-deoxyglucose (<sup>18</sup>F-FDG) has been widely used [22]. <sup>18</sup>F-FDG is reported to accumulate in macrophages, particularly M1-polarized macrophages in atherosclerotic lesions [23], which is similar to radiolabeled IgG behavior. Therefore, radiolabeled IgG would provide information similarly to <sup>18</sup>F-FDG in the diagnosis of atherosclerosis.

In this study, we found that IgG itself can be potentially used for the visualization of atherosclerotic plaques, especially atherosclerotic lesions in active inflammation independent of its target biomolecules. However, we also observed the high retention of radioactivities in blood 24 h after administration of <sup>99m</sup>Tc-TSP4-mAb (apoE<sup>-/-</sup>, 17.2 ± 2.1 %ID/g; WT, 17.2 ± 1.5 %ID/g), which were about three times higher than those in aortas. This may be because that IgG has a high molecular weight (about 150 kDa), which leads to a low rate of clearance from blood. To overcome this problem, the molecular weight of IgG should be decreased with its affinity to Fcγ receptors maintained. That is, an Fc fragment (about 50 kDa) obtained from IgG would be a suitable basic compound for atherosclerotic imaging. We are now developing an Fc fragment-based probe and evaluating to determine whether this probe can be used to visualize the inflammatory active areas of atherosclerotic lesions.



**Acknowledgments** This study was supported in part by MEXT KAKENHI (Grant Numbers: 24890003 and 26860961) and the Creation of Innovation Centers for Advanced Interdisciplinary Research Areas Program, Ministry of Education, Culture, Sports, Science and Technology, Japan.

**Open Access** This chapter is distributed under the terms of the Creative Commons Attribution-Noncommercial 2.5 License (<http://creativecommons.org/licenses/by-nc/2.5/>) which permits any noncommercial use, distribution, and reproduction in any medium, provided the original author(s) and source are credited.

The images or other third party material in this chapter are included in the work's Creative Commons license, unless indicated otherwise in the credit line; if such material is not included in the work's Creative Commons license and the respective action is not permitted by statutory regulation, users will need to obtain permission from the license holder to duplicate, adapt or reproduce the material.

## References

1. Ruberg FL, Leopold JA, Loscalzo J. Atherothrombosis: plaque instability and thrombogenesis. *Prog Cardiovasc Dis.* 2002;44:381–94.
2. Hanzawa H, Sakamoto T, Kaneko A, Manri N, Zhao Y, et al. Combined plasma and tissue proteomic study of atherogenic model mouse: approach to elucidate molecular determinants in atherosclerosis development. *J Proteome Res.* 2015;14:4257–69.
3. Stenina OI, Desai SY, Krukovets I, Kight K, Janigro D, Topol EJ, et al. Thrombospondin-4 and its variants: expression and differential effects on endothelial cells. *Circulation.* 2003;108:1514–9.
4. Frolova EG, Pluskota E, Krukovets I, Burke T, Drumm C, Smith JD, et al. Thrombospondin-4 regulates vascular inflammation and atherogenesis. *Circ Res.* 2010;107:1313–25.
5. Larson SM. Radiolabeled monoclonal anti-tumor antibodies in diagnosis and therapy. *J Nucl Med.* 1985;26:538–45.
6. Fischman AJ, Rubin RH, Khaw BA, Kramer PB, Wilkinson R, Ahmad M, et al. Radionuclide imaging of experimental atherosclerosis with nonspecific polyclonal immunoglobulin G. *J Nucl Med.* 1989;30:1095–100.
7. Abrams MJ, Juweid M, TenKate CI, Schwartz DA, Hauser MM, Gaul FE, et al. Technetium-99m-human polyclonal IgG radiolabeled via the hydrazino nicotinamide derivative for imaging focal sites of infection in rats. *J Nucl Med.* 1990;31:2022–8.
8. Ono M, Arano Y, Mukai T, Uehara T, Fujioka Y, Ogawa K, et al. Plasma protein binding of (99m)Tc-labeled hydrazino nicotinamide derivatized polypeptides and peptides. *Nucl Med Biol.* 2001;28:155–64.
9. Larsen SK, Solomon HF, Caldwell G, Abrams MJ. [99mTc]tricine: a useful precursor complex for the radiolabeling of hydrazinonicotinate protein conjugates. *Bioconjug Chem.* 1995;6:635–8.
10. Vucic E, Dickson SD, Calcagno C, Rudd JH, Moshier E, Hayashi K, et al. Pioglitazone modulates vascular inflammation in atherosclerotic rabbits noninvasive assessment with FDG-PET-CT and dynamic contrast-enhanced MR imaging. *JACC Cardiovasc Imaging.* 2011;4:1100–9.
11. Zhao Y, Kuge Y, Zhao S, Morita K, Inubushi M, Strauss HW, et al. Comparison of 99mTc-annexin A5 with 18F-FDG for the detection of atherosclerosis in ApoE<sup>-/-</sup> mice. *Eur J Nucl Med Mol Imaging.* 2007;34:1747–55.
12. Mantovani A, Sica A, Sozzani S, Allavena P, Vecchi A, Locati M. The chemokine system in diverse forms of macrophage activation and polarization. *Trends Immunol.* 2004;25:677–86.

13. Chinetti-Gbaguidi G, Baron M, Bouhlef MA, Vanhoutte J, Copin C, Sebti Y, et al. Human atherosclerotic plaque alternative macrophages display low cholesterol handling but high phagocytosis because of distinct activities of the PPARgamma and LXRalpha pathways. *Circ Res*. 2011;108:985–95.
14. Moore KJ, Sheedy FJ, Fisher EA. Macrophages in atherosclerosis: a dynamic balance. *Nat Rev Immunol*. 2013;13:709–21.
15. Shimizu Y, Hanzawa H, Zhao Y, Fukura S, Nishijima K, Sakamoto T, et al. Accumulation mechanism of non-targeted immunoglobulin G in atherosclerotic lesions. *J Nucl Med*. 2015;56 Suppl 3:462.
16. Ravetch JV, Bolland S. IgG Fc receptors. *Annu Rev Immunol*. 2001;19:275–90.
17. Hernandez-Vargas P, Ortiz-Munoz G, Lopez-Franco O, Suzuki Y, Gallego-Delgado J, Sanjuan G, et al. Fcgamma receptor deficiency confers protection against atherosclerosis in apolipoprotein E knockout mice. *Circ Res*. 2006;99:1188–96.
18. Temma T, Saji H. Radiolabeled probes for imaging of atherosclerotic plaques. *Am J Nucl Med Mol Imaging*. 2012;2:432–47.
19. Nakamura I, Hasegawa K, Wada Y, Hirase T, Node K, Watanabe Y. Detection of early stage atherosclerotic plaques using PET and CT fusion imaging targeting P-selectin in low density lipoprotein receptor-deficient mice. *Biochem Biophys Res Commun*. 2013;433:47–51.
20. Temma T, Ogawa Y, Kuge Y, Ishino S, Takai N, Nishigori K, et al. Tissue factor detection for selectively discriminating unstable plaques in an atherosclerotic rabbit model. *J Nucl Med*. 2010;51:1979–86.
21. Signore A, Prasad V, Malviya G. Monoclonal antibodies for diagnosis and therapy decision making in inflammation/infection. Foreword. *Q J Nucl Med Mol Imaging*. 2010;54:571–3.
22. Rudd JH, Warburton EA, Fryer TD, Jones HA, Clark JC, Antoun N, et al. Imaging atherosclerotic plaque inflammation with [18F]-fluorodeoxyglucose positron emission tomography. *Circulation*. 2002;105:2708–11.
23. Satomi T, Ogawa M, Mori I, Ishino S, Kubo K, Magata Y, et al. Comparison of contrast agents for atherosclerosis imaging using cultured macrophages: FDG versus ultrasmall superparamagnetic iron oxide. *J Nucl Med*. 2013;54:999–1004.